Desalination and Water Treatment
www.deswater.com

doi: 10.5004/dwt.2019.23777

156 (2019) 220–228
July

Performance of composite PES/MOF-5 membranes for the treatment of textile wastewater

G. Gnanaselvan[a,b], B. Sasikumar[a], G. Arthanareeswaran[a,*], Young Sun Mok[b,*]

[a]*Membrane Research Laboratory, Department of Chemical Engineering, National Institute of Technology, Tiruchirappalli-620015, India, email: gsel1033@gmail.com (G. Gnanaselvan), balaguru.sasikumar799@gmail.com (B. Sasikumar), Tel. +91431-2503118, Fax +91431-2500133, email: arthanaree10@yahoo.com (G. Arthanareeswaran)*
[b]*Department of Chemical and Biological Engineering, Jeju National University, Jeju 63243, Korea, Tel. +91431-2503118, Fax +91431-2500133, email: smokie@jejunu.ac.kr (Y.S. Mok)*

Received 14 September 2018; Accepted 12 January 2019

ABSTRACT

The composite polyethersulfone (PES) nanofiltration (NF) membranes were prepared by embedding metal organic framework (MOF-5) for the treatment of textile wastewater. Metal-organic frameworks are intensively explored as filler materials for polymeric membrane, predominantly as a result of their huge porosity, elegant pore size, and high polymer affinity. The hydrophilicity of PES/MOF-5 membranes has been enhanced due to the addition of MOF-5. The contact angle has been decreased from 73.1 to 60.3° and the pure water flux increased from 20.5 to 77.1 L/m² h at 0.75 wt. % loading of MOF-5. The incorporated PES/MOF-5 nanofiltration membranes had effective affinity for the removal of 97% and 89% for Methylene Blue (MB) and Indigo Carmine (IC) dyes respectively. In order to study adsorption performance of composite PES/MOF-5 membranes, the experiment of batch adsorption of textile dyes has been studied with the effect of pH. The improvement of membrane performances could be attributed to the well-tailored properties of MOF-5. This result shows that MOF-5 is the potential material for fabricating hybrid NF membranes for textile wastewater treatment.

Keywords: Textile wastewater; Metal-organic frameworks (MOFs); Membrane separation; Polyethersulfone (PES); Nanofiltration (NF)

1. Introduction

Effluents from various dye-utilizing industries are a global issue in the environmental concern. Industries like textile, plastic, paper, leather, food processing, and cosmetics contributed majorly to the discharge of dyes [1]. The effluent from textile industries contains organic and inorganic salts, heavy metals and dyes. Discharge of dye to hydrosphere can cause a serious problem because of their toxicity and carcinogenic effect on both aquatic and human life. Thus, it is essential to treat dye effluent before discharging them into the environment.

Numerous methods have been adopted for dye removal namely coagulation, adsorption [2], ion-exchange [3], electrochemical [4], oxidation, and membrane separation [5]. Membrane separation is an efficient method for treating dye effluent compared to other conventional methods because of its less energy consumption, effective removal percentage, higher selectivity, and easy handling process [6]. Nanofiltration (NF) was proven to be a promising technique for the removal of dyes from wastewater [5–7]. So, the consistent attempts have been made to fabricate novel membranes for wastewater treatment with high selectivity, permeability, and increased membrane stability. The performance of membranes could be enhanced by improving the interface compatibility of polymeric matrix and fillers. Cheng et al. [7] studied the incorporation of potential nanomaterials into membranes matrix improved the ultrafast molecular separation (UMS) membranes. The hydrophobic poly (vinylidene fluoride) (PVDF) membrane has been improved by the

*Corresponding author.

Presented at the InDA Conference 2018 (InDACON-2018), 20–21 April 2018, Tiruchirappalli, India

addition of mussel-inspired sticky catechol-functionalized poly (ethylene glycol) (Cate-PEG) [8]. X.H. Ma et al. [9] synthesized nanofiltration membranes by the incorporation of MOFs (NH_2-MIL-101(Al) and NH_2-MIL-101(Cr)) into chitosan polymeric matrix for the effective removal of multivalent cations. The MOFs is a good alternative compared to nano-fillers. Using MOFs as filler for enhancing the performance of polymeric membranes is a promising research area.

MOFs are broadly used in gas separation, gas storage, drug delivery, and catalysis [10]. MOFs exposed a potential adsorbent for water pollutants such as malachite green, methylene blue [11], copper ions [12] etc. MOFs have an advantage over other porous materials due to its high surface area, tunability, high porosity, and open metal sites etc [13]. Adsorptive removal of methyl orange and methylene blue dye has been investigated using MOF-235 and its shown that MOF can adsorb very large amount of dyes via electrostatic interaction between dyes and adsorbent [14]. Echaide et al. studied the performance of MOFs embedded nanocomposite membranes for the removal of dye with different solvent [15]. However, studies on MOFs as an adsorbent and its effects on membranes synthesis for liquid phase separation are limited. PES is selected for nanofiltration membrane due to its good chemical, thermal and mechanical stability, commercial availability, effective selectivity, and permeability [18–20].

In accordance with aforementioned, in the present work detailed investigation was carried out for the removal of MB and IC using MOF-5 incorporated PES nanofiltration membranes. We have studied the incorporation of MOF-5 into polymeric membranes is an effective material for removal of hazardous materials like Cu (II) and Co (II) from wastewater [16]. The effect of MOF-5 on the membrane morphology and performance was evaluated. The effectiveness of MOF-5 incorporated membranes for dye removal was studied through integrated adsorption and nanofiltration process. Chemical structures of dye used for adsorption and filtration studies are shown in Fig. 1.

2. Materials and methods

PES (Grade 3000P) was bought from M/s. Solvay Process, India, Ltd. N,N-dimethylformamide was procured from Alfa Aesar, USA. Terephthalic acid was purchased from SRL Pvt Ltd., India, Zinc nitrate hexahydrate was acquired from Loba Chemie Pvt Ltd, India. Indigo carmine (M.W: 466) and methylene blue dye (M.W: 319) were obtained from SRL Pvt Ltd, Mumbai, India. Distilled water produced using a double distillation unit in the laboratory.

2.1. Membrane preparation

MOF-5 has been synthesized by the described procedure in the literature [16,17]. The phase inversion methods have been used in the fabrication of neat and MOF-5 incorporated PES membranes. MOF-5 loading was kept at 0.25%, 0.5% and 0.75% of PES. The casting solutions contain 17.5% of PES and MOF-5 and 21.7 ml (82.5%) of DMF solvent. The composition of membrane casting solution listed in Table 1. For composite membranes the MOF-5 particles were added into DMF solution and well dispersion by ultra-sonication for 1 h, followed by stirring at room temperature. The PES powder added into the mixture solution and stirred for 3–5 h until a uniform dispersion occurred. After the complete dispersion, the dope solution placed for 30 min in ultra-sonication for the preparation of homogenous casting solution. For neat PES, same procedure followed for the preparation of dope solution without adding the MOF-5 particles. The above-prepared dope solution cast by 400 µm thickness of casting knife at smooth glass plate. After casting, the thin film instantly immersed in the distilled water at 10°C. The synthesized PES membrane submerged into fresh distilled water for 24 h to remove the residual solvent.

2.2. Membrane characterisation

2.2.1. FTIR analysis

FTIR spectroscopic investigation of Neat PES and PES/MOF-5 membranes was analyzed by the attenuated total reflection (ATR-FTIR) technique using Thermo Fisher Scientific Nicolet i5S FTIR analyzer (Thermo Nicolet Cor-

Table 1
The composition of membranes casting solution

Membrane code	PES and MOF-5 composition (17.5 wt %)	Solvent (wt %)	
	PES	MOF-5	DMF
M0	100%	–	82.5%
M1	99.75%	0.25%	82.5%
M2	99.50%	0.50%	82.5%
M3	99.25%	0.75%	82.5%

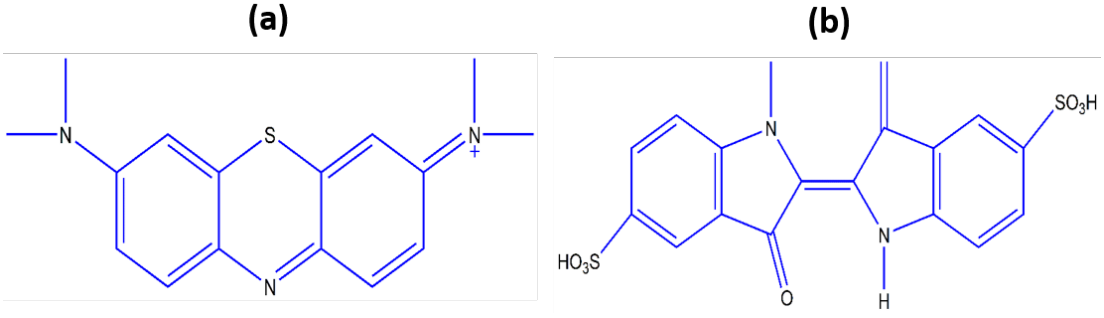

Fig. 1. Structures of dye used for adsorption and filtration studies. (a) Methylene Blue (b) Indigo Carmine.

poration, USA). The change in chemical structure can be observed using wavenumber drift against the percentage transmittance, and the samples were analyzed over the spectral region of wavelengths from 400 to 4000 cm^{-1}.

2.2.2. XRD analysis

XRD spectra of Neat PES and PES/MOF-5 membranes were analyzed by X-ray diffractometer (Model D8 advance, Bruker, Germany) by the monochromatic source of Cu Ka radiation. The membrane samples were operated in 5-55° angle for 2 h under 40 kV of an acceleration voltage.

2.2.3. Surface morphology

The structural morphology of neat PES and PES/MOF-5 membranes were analyzed by Scanning Electron Microscope (VEGA 3, TESCAN, USA). The membrane pieces were frozen and broken using liquid nitrogen. The membranes samples were gold coated by sputtering to make them conductive. The distribution of MOF-5 on PES/MOF-5 membranes, examined by energy dispersion of X-ray (EDX, S250, and EDAX).

2.2.4. Contact angle measurement

The surface hydrophilicity of composite PES/MOF-5 and neat PES membranes were investigated by contact angle measurement using a goniometer (model 250-F1 Rame-Hart Instruments, Succasunna, NJ). The experiment followed the sessile drop technique. The contact angle values were measured from the average value of the individual droplets in the five regions of the membrane surface. Contact angle measurement determines the hydrophilicity of membranes.

2.2.5. Thermogravimetric analysis (TGA)

The TGA analysis of the modified and unmodified PES membranes was conducted by a thermogravimetric analyzer (DGT 2000, Perkin Elmer, USA). The membrane pieces were kept at 60°C in a vacuum oven for the removal of moisture content. The experiment was performed with the temperature range of 50–700°C under a nitrogen atmosphere with a heating rate of 10°C/min.

2.3. Permeation studies

The permeation of composite PES/MOF-5 and neat PES membranes were studied for both pure water and 50 mg/l concentration of textile dye (methylene blue and indigo carmine) at 10 bar pressure with three different pH values such as 3 (highly acidic), 7 (neutral), 11 (highly basic) by using dead-end Nanofiltration cell (model HP4750 STIRRED CELL, USA) with effective membrane area of 14.6 cm^2. Initially, membranes were compacted to collect steady state permeate volume. Once a steady state was reached, the membrane permeate volume was collected for every 10 min. The membranes permeate flux (J_w) was studied by the following equation.

$$j_w = \frac{V}{A * \Delta t} \tag{1}$$

where J_w - pure water flux (L/m^2 h), V - permeate volume (L), A - effective membrane area (m^2), Δt - permeation time (h).

2.4. Membrane porosity and pore size

To study the porosity and pore size of neat PES and composite PES/MOF-5 membranes, the samples were cut into specific sizes and noting their wet weight and the membranes sample were placed in an oven at a temperature of 60°C for 24 h. The membrane porosity (ε) was calculated by the following Eq. (2).

$$\varepsilon = \left(\frac{\frac{\omega_1 - \omega_2}{d_w}}{\frac{(\omega_1 - \omega_2)}{d_w} + \left(\frac{\omega_2}{d_p} \right)} \right) \tag{2}$$

where ω_1 - membrane wet weight (g), ω_2 - membrane dry weight (g), d_w -density of the water (kg/cm^3), d_p - density of the polymer (kg/cm^3).

The average pore radius of membranes was calculated by Guerout– Elford–Ferry equation [18].

$$r_m = \sqrt{\left(\frac{(2.9 - 1.75\varepsilon) 8Ql\eta}{\varepsilon\, A\, \Delta P} \right)} \tag{3}$$

where Q - flow rate of the permeate (m^3/s), A - effective area of the membrane (m^2), ΔP - transmembrane pressure (Pa), η - dynamic viscosity of the water (Pa s), l - thickness of the membrane (m).

2.5. Rejection of textile dye

The rejection percentage of textile dye such as methylene blue (λ = 668 nm) and indigo carmine (λ = 610 nm) for both neat PES and PES/MOF-5 membranes were calculated by the following Eq. (4). The feed and permeate concentration of textile dye solution has been analysed by a UV visible spectrophotometer (Model: spectroquant prove 600).

$$R = \left(1 - \frac{C_f}{C_p} \right) \times 100 \tag{4}$$

where C_f - feed concentrations of the dye solutions, C_p - permeate concentrations of the dye solutions.

2.6. Batch adsorption studies of dyes

The batch adsorption studies of methylene blue and indigo carmine dyes of neat PES and PES/MOF-5 membranes were performed. 2 cm × 2 cm of membranes were cut into pieces and kept in an airtight bottle filled with dyes (50 mg/l) of 40 ml with varying pH such 3 pH, 7 pH, and 11 pH by using a rotary shaker with the 250 rpm at 30°C for 24 h. The dye removal percentage calculated by the following equation.

$$Dye\ removal\ \% = \frac{C_o - C_q}{C_o} \times 100 \quad (5)$$

where C_o - initial concentration of dye, C_q - final concentration of dye

3. Results and discussion

3.1. FTIR analysis

The membranes FTIR spectra confirm the effectiveness of incorporation of MOF-5 into the PES membrane, as shown in Fig. 2. The FTIR spectra illustrate the expected spectrums of PES membranes at 1578 cm^{-1} (aromatic bands of benzene ring), 1485 cm^{-1} (C–C bond stretch) and 1248 cm^{-1} (aromatic ether band) [19]. The MOF-5 incorporated PES membranes have the spectrum at 3370 cm^{-1}, which is associated with the band of O-H stretching, indicating that the MOF-5 incorporation and presence in an integral part of PES membrane.

3.2. XRD analysis

Fig. 3 shows the XRD patterns of neat and MOF-5 embedded PES membranes and MOF-5. Both neat and PES/MOF-5 membranes have the peak occurrence at 2θ = 18°, which indicate the amorphous characteristic of PES, confirming the successful fabrication of PES membranes [20]. The XRD spectra of MOF-5 at 6.9° and 9.8° at 2θ indicate the successful MOF-5 fabrication [21]. The peak at 2θ = 6.9° in the PES/ MOF-5 membranes has shifted a little, which indicate the distribution of MOF-5 in the PES matrix. The appearance of these peaks clearly shows that MOF-5 acts as a surface modifying agent for PES membranes and proves the MOF-5 and PES matrix interaction [18].

3.3. Surface morphology

Cross-section images of composite PES/MOF-5 and neat PES and membranes are shown in Fig. 4. The asymmetry with a finger-like structure occurred in both neat PES and PES/MOF-5 membranes. The interconnection between the bottom layer and skin top layer were improved for PES/MOF-5 membranes. Finger-like substructures and thin skin layer were observed with the addition of MOF-5. The permeability and pore radius was increased. The wide finger like pore size and macro voids of membranes were enlarged in the bottom layer with increasing the concentration of MOF-5 into PES matrix, which would improve the pore size and permeability of PES membranes [22].

3.4. EDX analysis

Fig. 5 shows the EDX spectra of hybrid PES/MOF-5 and neat PES membranes. It shows that all the organic compound has been present in neat PES membrane as well as PES/MOF-5 membranes and MOF-5 distribution on PES matrix. The presence of Zn(II) element has proved the impact of MOF-5 into the PES/MOF-5. The minor percentage of Zn(II) in the PES/MOF-5 membranes due to the low loading of MOF-5 into the PES matrix [23].

3.5. Contact angle measurement

The membranes permeability and antifouling property always depended upon the hydrophilic nature of membranes, which is commonly investigated via contact angle measurement. Contact angle measurement of neat PES and PES/MOF-5 membranes are summarized in Table 2. When increasing the loading percentage of MOF-5 into PES matrix the water contact angle decreased from 73.1 to 60.3° which indicate that the hydrophilicity and pore radius of PES membranes increased. The hydrophilicity of PES/MOF-5 membranes has enhanced with the hydrophilic hydroxyl (–OH) functional group (MOF-5) incorporation into the polymer matrix (PES membranes) [24]. It clearly proves that the incorporation of MOF-5 has enhanced the antifouling property and permeability of PES matrix [25].

3.6. Thermogravimetric analysis

Fig. 6 shows the thermogravimetric analysis of composite PES/MOF-5 and neat PES membranes. Thermo-

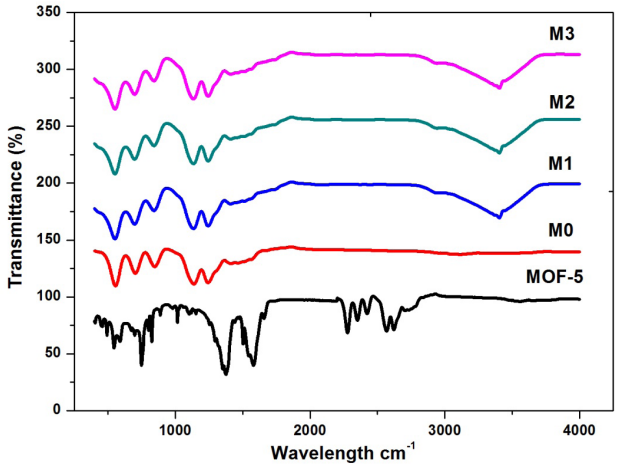

Fig. 2. FTIR spectra of membranes.

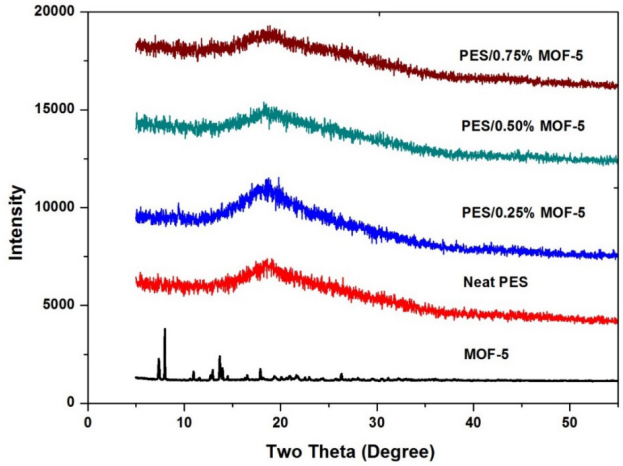

Fig. 3. XRD analysis of membranes.

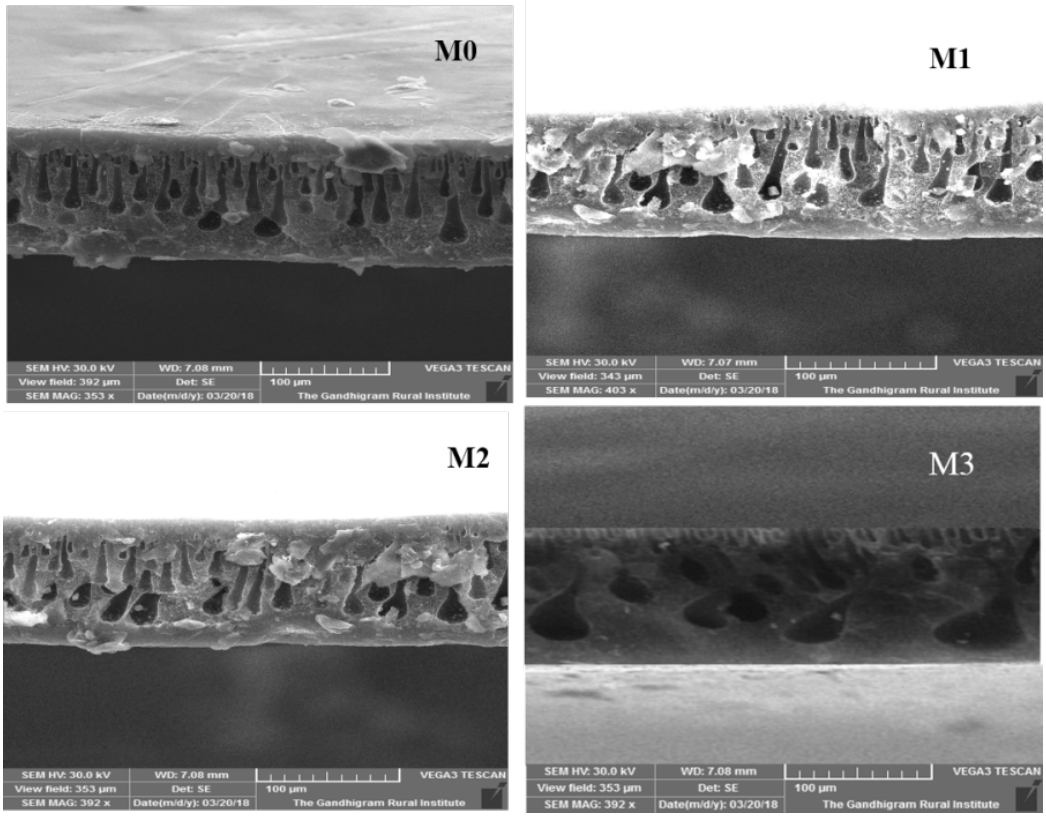

Fig. 4. Cross-sectional image of membranes.

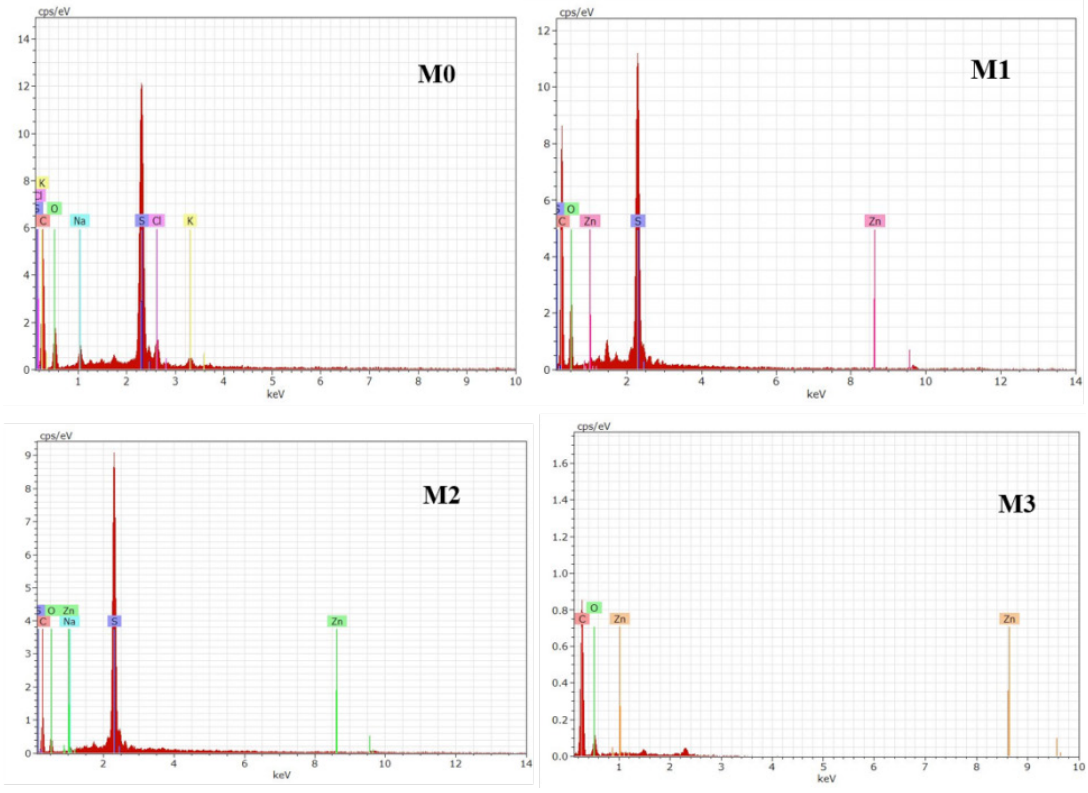

Fig. 5. EDX image of membranes.

Table 2
The porosity, pore size and contact angle of membranes

Sl. no	Name of the membranes	Porosity (%)	Pore radius (nm)	Water contact angle (°)
1	M0	63.40	6.45	73.1 ± 2.3
2	M1	64.96	6.91	70.6 ± 1.7
3	M2	66.67	7.74	66.7 ± 2.1
4	M3	67.40	8.05	60.3 ± 2.5

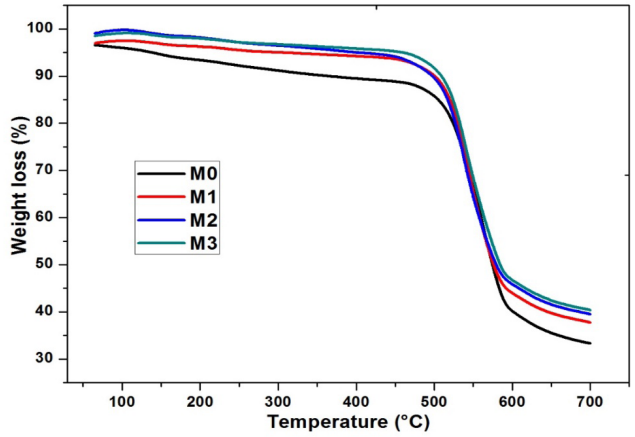

Fig. 6. TGA Analysis of membranes.

graph of unmodified PES membranes has two weight losses, below 100°C, the primary weight loss occurred due to the evaporation of water molecules. From 100 to 470°C the second weight loss arose by reason of the decomposition of PES membranes. Three stages of thermal degradation occurred in MOF-5 incorporated PES membranes. Below 100°C, the first stage of thermal degradation occurred due to the water loss. The second stage of thermal degradation occurred in between 100 to 450°C due to the degradation of MOF-5. At the third stage, major weight losses occurred due to the degradation of PES membranes. The TGA curves confirm that MOF-5 incorporation into PES matrix which enhances the thermal stability of membranes with increasing the concentration of MOF-5 and this could be due the good interfacial compatibility between MOF-5 and PES matrix [26–28].

3.7. Porosity and pore size of membranes

The porosity and pore size of the MOF-5 modified and unmodified PES membranes were shown in Table 2. The porosity of the MOF-5 incorporated PES membranes was increasing from 63.4 to 67.4% with the increasing concentration of MOF-5 into the PES membranes. Increasing porosity of the membranes impact to the antifouling properties of membranes [29]. The pore size of the membranes is gradually increasing from 6.45 to 8.05 nm with the increasing concentration of MOF-5. The formation of a pore in the surface of the membrane enhances the permeability and adsorption of membranes [30].

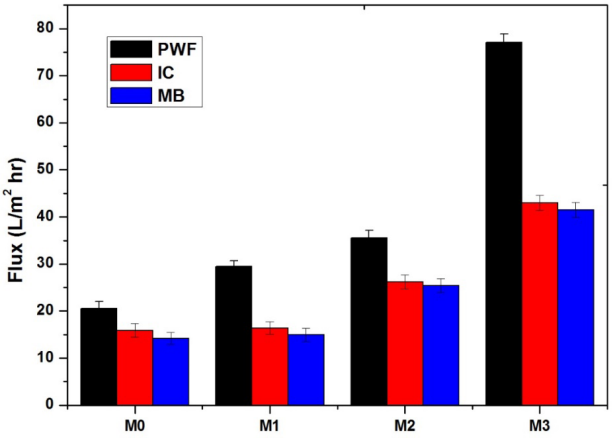

Fig. 7. Permeate flux rate of membranes.

3.8. Permeability of membranes

Fig. 7 shows the permeability of pure water and dye solution of membranes. The pure water permeation of PES/MOF-5 membranes was increasing from 20.5 to 77.1 L/m^2 h compared to neat PES membranes. The permeability of PES membranes was influenced by the concentration of MOF-5 into PES matrix. It confirms that the hydrophilicity and pore formation of PES membranes were effectively enhanced by the addition of MOF-5. The permeate flux of dye solution also increased compared to neat PES membranes but the pure water flux is high compared to dye solution flux due to the fouling formation on the membranes. The particles agglomeration occurred in the PES/MOF-5 membranes when increasing the MOF-5 particles concentration more than 0.75% which leads to the particles irregular distribution in the composite membranes [31]. The membrane permeability clearly shows that incorporation of MOF-5 into PES matrix to enhance the hydrophilicity and anti-fouling properties of nanofiltration membranes [32].

3.9. Dye rejection

The percentage rejection of textile dye (Methylene Blue and Indigo Carmine) has been studied for both neat PES and PES/MOF-5. Figs. 8 and 9 show the rejection percentage of Methylene blue and Indigo carmine respectively. The MOF-5 incorporated PES membranes have higher rejection percentage of methylene blue and indigo carmine compared to neat PES membranes. The modified PES membranes have higher rejection such as 97% and 89% for MB and IC respectively. The selectivity for dyes removal has been enhanced due to the coordination interactions between polymeric matrix (PES) functional groups and/or organic ligands and Zn(II) [31]. The high rejection percentage of IC dyes due to the size exclusion and charge repulsion [33]. The rejection performance of MB and IC for PES/MOF-5 membranes increased with increasing concentration of MOF-5 into PES matrix [32]. The presence of metal oxide in the MOF-5 has enhanced the higher adsorption of dye on PES membranes. MB dye has a higher rejection percentage due to the electrostatic attraction of positively charged MB with negative charged PES matrix [34].

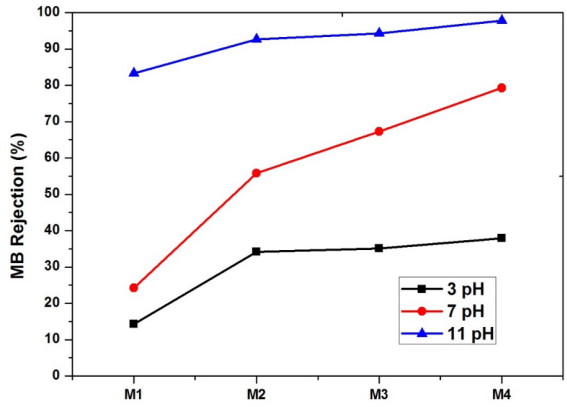

Fig. 8. Rejection percentage of Methylene Blue.

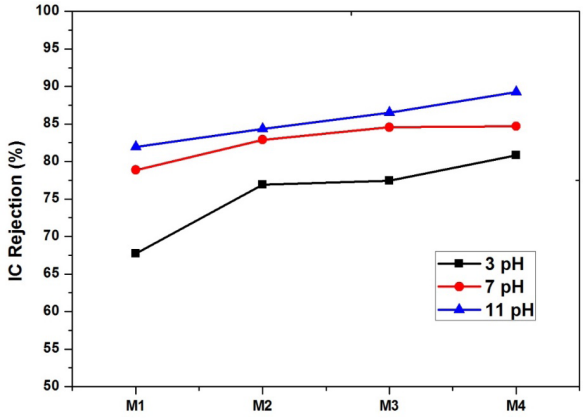

Fig. 9. Rejection percentage of Indigo Carmine.

3.10. Effect of pH

Changing pH of the textile dyes feed solution plays a vital role in the rejection of textile dyes. At 3 pH the rejection percentage of methylene blue increasing from 14.2 to 37.8%. At 7 pH the rejection increasing from 24.2 to 79.2%. For 11 pH the rejection of effluent increasing from 83 to 97%. For indigo carmine, the rejection percentage increasing from 67.7 to 80% for 3 pH. For 7 pH the rejection increasing from 78.8 to 84.7% For 11 pH the rejection of effluent increasing from 81 to 89%. When increasing the pH of the effluent, the rejection percentage also increasing for MOF-5 incorporated PES membranes. The metal oxide of MOF-5 provides the effective binding site which enhances adsorption of Methylene blue and Indigo carmine on PES/MOF-5 membranes. When increasing the pH, the textile dye highly adsorbed on the membranes which improve the rejection percentage [34].

3.11. Batch adsorption study

3.11.1. Rejection of methylene blue dye

The adsorptive removal of methylene blue dye on neat PES and PES/MOF-5 membranes with varying pH of the feed solution is shown in Fig. 10. The rejection percentage of MB increased from 74.6 to 82.4%. With increasing concentration of MOF-5 into PES membranes, the rejection of MB dye also increased due to the interaction between the MB and Zn(II). From this adsorption study, the MOF-5 incorporated PES membranes have high adsorption which leads to the high rejection of Dye compared to neat PES membranes. Rejection percentage of MB has effectively increased when increasing the pH of the feed solution [34].

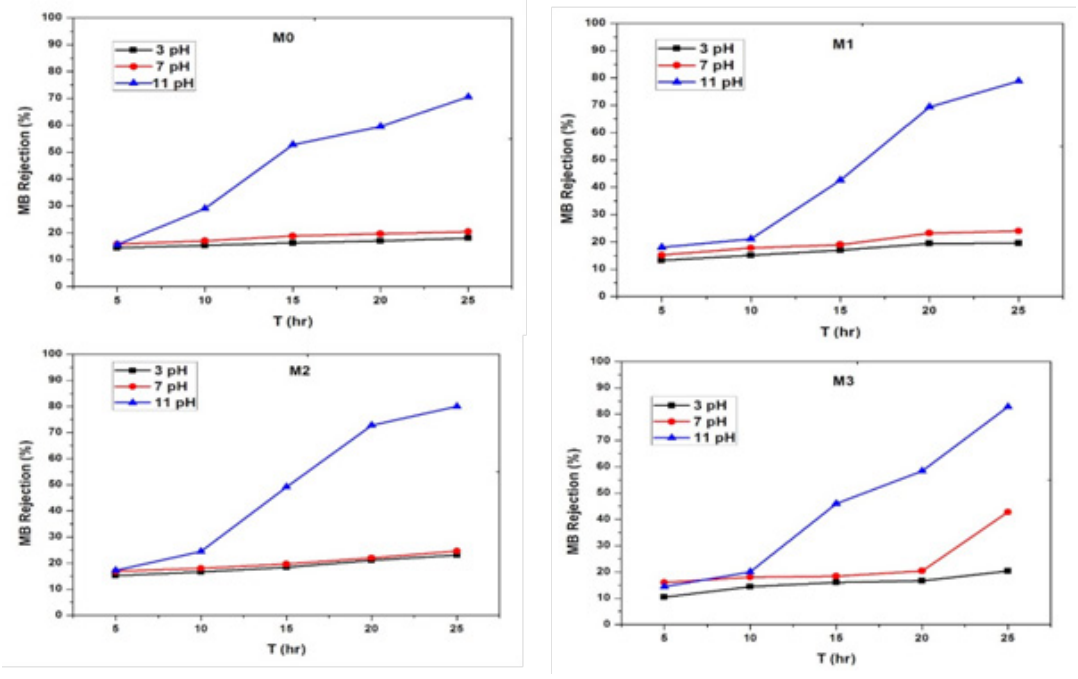

Fig. 10. Methylene blue rejection (%) by adsorption of membranes.

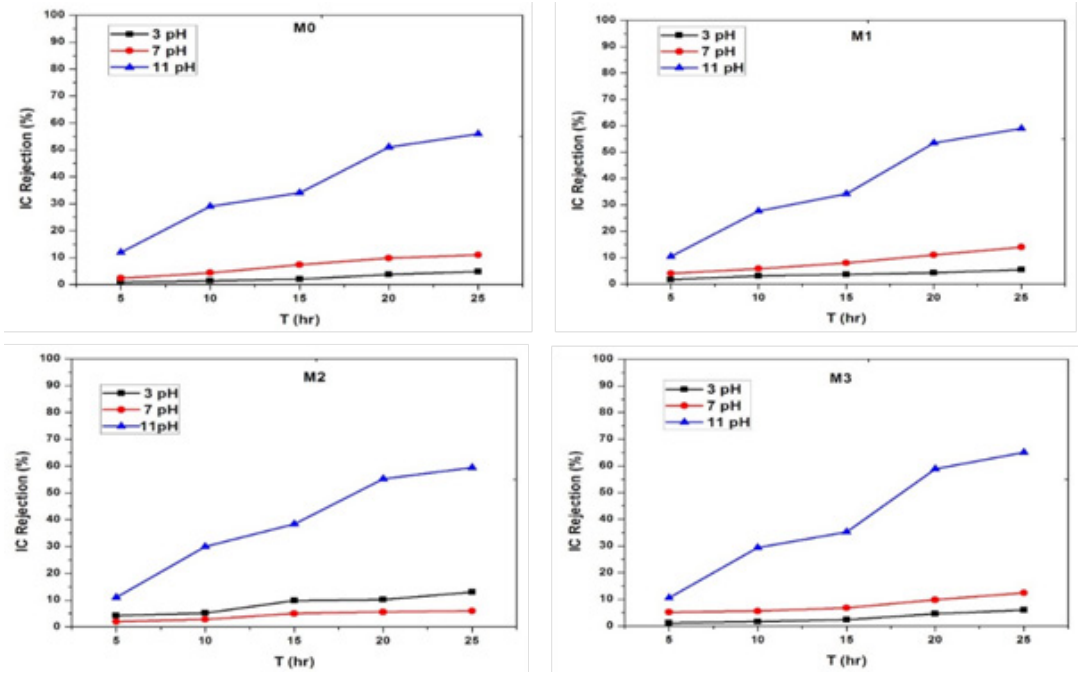

Fig. 11. Indigo Carmine rejection (%) by adsorption of membranes.

3.11.2. Removal of indigo carmine dye

The adsorptive removal of indigo carmine dye on neat PES and PES/MOF-5 membranes with varying pH of the feed solution is shown in Fig. 11. For indigo carmine, the rejection percentage by adsorption has been increasing from 56 to 65%. The removal percentage has been increasing with increasing concentration of MOF-5 in the PES/MOF-5 membranes. IC dye has less rejection percentage compared to MB dye due to the size exclusion [33].

4. Conclusion

The prepared neat PES and MOF-5 incorporated PES membranes were characterized by FTIR, XRD, SEM with EDX and TGA. All the results confirm the impact of MOF-5 into PES matrix. Incorporation of MOF-5 in the PES matrix influenced the porosity and pore size of the fabricated composite PES/MOF-5 membranes. Further, the contact angle of composite membranes decreasing from 73.1 to 60.3° due to the improvement of hydrophilicity and permeability of composite PES/MOF-5 membranes were enhanced from 20.5 to 77.1 L/m^2 h due to the metal clusters of MOF-5. The incorporated PES/MOF-5 nanofiltration membranes had effective affinity for the removal of 97% and 89% for Methylene Blue (MB) and Indigo Carmine (IC) dyes respectively. PES/MOF-5 membranes have high rejection percentage of textile dye compared to neat PES membrane. Dye adsorption properties of PES/MOF-5 membranes were enhanced due to the coordination interaction between the dye and Zn(II) presence in the MOF-5. Methylene blue dye has a high rejection percentage compare to indigo carmine. In the batch adsorption process, the MOF-5 incorporated PES membrane has high removal percentage of dye, which increased with increasing concentration of MOF-5 into PES matrix. The PES/MOF-5 membrane is a potential material for the treatment of textile wastewater.

References

[1] S. Yu, M. Liu, M. Ma, M. Qi, Z. Lü, C. Gao, Impacts of membrane properties on reactive dye removal from dye/salt mixtures by asymmetric cellulose acetate and composite polyamide nanofiltration membranes, J. Membr. Sci., 350 (2010) 83–91.
[2] N.M. Mahmoodi, Synthesis of core-shell magnetic adsorbent nanoparticle and selectivity analysis for binary system dye removal, J. Ind. Eng. Chem., 20 (2014) 2050–2058.
[3] L. Xu, L.S. Du, C. Wang, W. Xu, Nanofiltration coupled with electrolytic oxidation in treating simulated dye wastewater, J. Membr. Sci., 409–410 (2012) 329–334.
[4] V.S. Antonin, S. Garcia-Segura, M.C. Santos, E. Brillas, Degradation of Evans Blue diazo dye by electrochemical processes based on Fenton's reaction chemistry, J. Electroanal. Chem., 747 (2015) 1–11.
[5] A. Akbari, S. Desclaux, J.C. Rouch, J.C. Remigy, Application of nanofiltration hollow fibre membranes, developed by photografting, to treatment of anionic dye solutions, J. Membr. Sci., 297 (2007) 243–252.
[6] S.S. Shenvi, A.M. Isloor, A.F. Ismail, S.J. Shilton, A. Al Ahmed, Humic acid based biopolymeric membrane for effective removal of Methylene Blue and Rhodamine B, Ind. Eng. Chem. Res., 54 (2015) 4965–4975.
[7] X.Q. Cheng, Z.X. Wang, X. Jiang, T. Li, C.H. Lau, Z. Guo, J. Ma, L. Shao, Towards sustainable ultrafast molecular-separation membranes: From conventional polymers to emerging materials, Prog. Mater. Sci., 92 (2018) 258–283.
[8] H. Sun, X. Yang, Y. Zhang, X. Cheng, Y. Xu, Y. Bai, L. Shao, Segregation-induced in situ hydrophilic modification of poly (vinylidene fluoride) ultrafiltration membranes via sticky poly (ethylene glycol) blending, J. Membr. Sci., 563 (2018) 22–30.
[9] X.H. Ma, Z. Yang, Z.K. Yao, Z.L. Xu, C.Y. Tang, A facile preparation of novel positively charged MOF/chitosan nanofiltration membranes, J. Membr. Sci., 525 (2017) 269–276.

[10] H. Ting, H.Y. Chi, C.H. Lam, K.Y. Chan, D.Y. Kang, High-permeance metal-organic framework-based membrane adsorber for the removal of dye molecules in aqueous phase, Environ. Sci. Nano., 4 (2017) 2205–2214.
[11] E. Haque, J.E. Lee, I.T. Jang, Y.K. Hwang, J.S. Chang, J. Jegal, S.H. Jhung, Adsorptive removal of methyl orange from aqueous solution with metal-organic frameworks, porous chromium-benzenedicarboxylates, J. Hazard. Mater., 181 (2010) 535–542.
[12] N. Bakhtiari, S. Azizian, Adsorption of copper ion from aqueous solution by nanoporous MOF-5: A kinetic and equilibrium study, J. Mol. Liq., 206 (2015) 114–118.
[13] J. Abdi, M. Vossoughi, N.M. Mahmoodi, I. Alemzadeh, Synthesis of metal-organic framework hybrid nanocomposites based on GO and CNT with high adsorption capacity for dye removal, Chem. Eng. J., 326 (2017) 1145–1158.
[14] E. Haque, J.W. Jun, S.H. Jhung, Adsorptive removal of methyl orange and methylene blue from aqueous solution with a metal-organic framework material, iron terephthalate (MOF-235), J. Hazard. Mater., 185 (2011) 507–511.
[15] C. Echaide-Górriz, S. Sorribas, C. Téllez, J. Coronas, MOF nanoparticles of MIL-68(Al), MIL-101(Cr) and ZIF-11 for thin film nanocomposite organic solvent nanofiltration membranes, RSC Adv., 6 (2016) 90417–90426.
[16] G. Gnanasekaran, S. Balaguru, A. Gangasalam, D.B. Das, Removal of hazardous material from wastewater by using metal organic framework (MOF) -embedded polymeric membranes removal of hazardous material from wastewater by using metal organic framework (MOF) - embedded polymeric membranes, Sep. Sci. Technol., 00 (2018) 0–13. doi:10.1080/01496395.2018.1508232.
[17] N. Bakhtiari, S. Azizian, Adsorption of copper ion from aqueous solution by nanoporous MOF-5 : A kinetic and equilibrium study, 206 (2015) 114–118.
[18] J.F. Li, Z.L. Xu, H. Yang, L.Y. Yu, M. Liu, Effect of TiO_2 nanoparticles on the surface morphology and performance of microporous PES membrane, Appl. Surf. Sci., 255 (2009) 4725–4732.
[19] A. Rahimpour, UV photo-grafting of hydrophilic monomers onto the surface of nano-porous PES membranes for improving surface properties, 265 (2011) 93–101.
[20] A. Ananth, G. Arthanareeswaran, H. Wang, The influence of tetraethylorthosilicate and polyethyleneimine on the performance of polyethersulfone membranes, Desalination, 287 (2012) 61–70.
[21] S. Ahmad, A. Badshah, H. Muhammad, M. Jawad, S. Mustansar, U. Ali, S.U. Khan, Synthesis of highly stable MOF-5 @ MWCNTs nanocomposite with improved hydrophobic properties, (2017).
[22] F. Gholami, S. Zinadini, A.A. Zinatizadeh, A.R. Abbasi, TMU-5 metal-organic frameworks (MOFs) as a novel nanofiller for flux increment and fouling mitigation in PES ultrafiltration membrane, Sep. Purif. Technol., 194 (2018) 272–280.
[23] L. Shen, X. Bian, X. Lu, L. Shi, Z. Liu, L. Chen, Z. Hou, K. Fan, Preparation and characterization of ZnO/polyethersulfone (PES) hybrid membranes, Desalination, 293 (2019) 21–29.
[24] F. Gholami, S. Zinadini, A.A. Zinatizadeh, A.R. Abbasi, TMU-5 metal-organic frameworks (MOFs) as a novel nano filler for flux increment and fouling mitigation in PES ultrafiltration membrane, Separ. Purif. Technol., 194 (2018) 272–280.
[25] V. Vatanpour, S.S. Madaeni, R. Moradian, S. Zinadini, B. Astinchap, Fabrication and characterization of novel antifouling nanofiltration membrane prepared from oxidized multiwalled carbon nanotube/polyethersulfone nanocomposite, J. Membr. Sci., 375 (2011) 284–294.
[26] R. Sathish Kumar, G. Arthanareeswaran, Y. Lukka Thuyavan, I. A.F., Enhancement of permeability and antibiofouling properties of polyethersulfone (PES) membrane through incorporation of quorum sensing inhibition (QSI) compound, J. Taiwan Inst. Chem. Eng., 72 (2017) 200–212.
[27] S. Sorribas, P. Gorgojo, C. Tellez, J. Coronas, A.G. Livingston, High flux thin film nanocomposite membranes based on MOFs for organic solvent nanofiltration High flux thin film nanocomposite membranes based on MOFs for organic solvent nanofiltration, J. Amer. Chem. Soc., 135(40) (2013) 15201–15208.
[28] P.D. Sutrisna, J. Hou, M.Y. Zulkifli, H. Li, Y. Zhang, W. Liang, D.M. D'Alessandro, V. Chen, Surface functionalized UiO-66/Pebax-based ultrathin composite hollow fiber gas separation membranes, J. Mater. Chem. A., 6 (2018) 918–931.
[29] H.P. Srivastava, G. Arthanareeswaran, N. Anantharaman, V.M. Starov, Performance of modified poly(vinylidene fluoride) membrane for textile wastewater ultrafiltration, Desalination, 282 (2011) 87–94.
[30] R. Sathish Kumar, G. Arthanareeswaran, D. Paul, J.H. Kweon, Effective removal of humic acid using xanthan gum incorporated polyethersulfone membranes, Ecotoxicol. Environ. Saf., 121 (2015) 223–228.
[31] R. Zhang, S. Ji, N. Wang, L. Wang, G. Zhang, J.R. Li, Coordination-driven in situ self-assembly strategy for the preparation of metal-organic framework hybrid membranes, Angew. Chemie - Int. Ed., 53 (2014) 9775–9779.
[32] J. Babu, Z.V.P. Murthy, Treatment of textile dyes containing wastewaters with PES/PVA thin film composite nanofiltration membranes, Sep. Purif. Technol., 183 (2017) 66–72.
[33] J. Gao, Z. Thong, K. Yu Wang, T.S. Chung, Fabrication of loose inner-selective polyethersulfone (PES) hollow fibers by one-step spinning process for nanofiltration (NF) of textile dyes, J. Membr. Sci., 541 (2017) 413–424.
[34] L. Zheng, Y. Su, L. Wang, Z. Jiang, Adsorption and recovery of methylene blue from aqueous solution through ultrafiltration technique, Sep. Purif. Technol., 68 (2009) 244–249.